The evaluation of mixing methods in HYSPLIT using measurements from controlled tracer experiments

Fong Ngan[1,2], Christopher P. Loughner[1,2,3], and Ariel Stein[1]

[1]*Air Resources Laboratory, National Oceanic Atmospheric Administration, College Park, Maryland*

[2]*Cooperative Institute for Satellite Earth System Studies, University of Maryland, College Park, Maryland*

[3]*Earth System Science Interdisciplinary Center, University of Maryland, College Park, Maryland*

Manuscript submitted to

Atmospheric Environment

Corresponding author: Fong Ngan, 5830 University Research Court., NCWCP Rm 4207, College Park, MD 20740, Phone: 301-683-1375, E-mail: Fantine.Ngan@noaa.gov

Abstract

The HYSPLIT dispersion model has different options to estimate the turbulent mixing depending on the availability of stability and turbulent parameters in the meteorological data. Dispersion simulations using different mixing options were conducted to simulate two controlled tracer experiments – the Project Sagebrush phase 1 (PSB1) for the sub-kilometer transport and the Cross Appalachian Tracer Experiment (CAPTEX) for the long-range transport. Through the comparisons of velocity variance and the evaluations of tracer concentrations, we evaluated different estimations of the turbulent velocity variance affecting the dispersion results. The mixing options in HYSPLIT are the Belijaars-Holtslag (BH) method, the Kantha-Clayson (KC) method, the turbulent kinetic energy (TKED) option, and the turbulent exchange coefficient (EXCH) option. The KC and EXCH method produced a larger maximum of the vertical velocity variance and at a higher altitude than other mixing options did. The vertical velocity variance profile of the BH scheme had a sharp increase from the surface to the height of the maximum values. The TKED option generated a flat profile with the smallest variation in its value with height. The plumes generated by the BH and TKED method (weaker mixing) had higher concentrations near the surface than those driven by the KC and EXCH option (stronger mixing). The statistical rank for the dispersion result using the TKED option was slightly better than others while the BH mixing generated results with a roughly worse rank. No mixing option always outperformed the other options. HYSPLIT users can select a mixing option according to the scenario and availability of meteorological fields, and use different options to generate dispersion ensembles.

Keywords: HYSPLIT, dispersion, PSB1, CAPTEX, turbulent velocity variance

1. Introduction

To simulate the movement of pollutants in the atmosphere, a Lagrangian model simulates the emission by releasing many particles at the source location over a period of time. By adding a random component according to the dispersive nature of the atmosphere to the advective motion of each particle, the particles released at the source will be transported and mixed in space and time (Draxler and Hess, 1998). The turbulent component of the process is the product of the computer-generated random number and the standard deviation of the turbulent velocity. HYSPLIT, the dispersion model developed by the National Oceanic and Atmospheric Administration Air Resource Laboratory, uses regional and global products from various numerical weather models – the Weather Research and Forecasting (WRF; Powers et al. 2017) model, the Global Forecast System (GFS; Kanamitsu, 1989) model, the Modern-Era Retrospective analysis for Research and Applications (MERRA; Rienecker et al. 2011), the European Center for Medium-Range Weather Forecasts (ECMWF; Dee et al. 2011), etc. Depending on the availability of stability and turbulent parameters in the meteorological data used to drive the dispersion simulation, users can choose different options in HYSPLIT to estimate the turbulent velocity variances (Stein et al. 2015). The estimation can be based on the stability function diagnosed from other meteorological variables such as friction velocity and mixing height. If the meteorological model does not provide them, temperature and wind soundings are used to diagnose the boundary layer stability parameters. Other methods include using the total turbulent kinetic energy (TKE) or mixing diffusivity to calculate the standard deviation of turbulent velocity (Draxler and Hess, 1997).

The main goal of this study is to understand the mixing characteristics generated by different estimations of the turbulent velocity variance affecting the dispersion results. Toward this aim, we conducted meteorological simulations with the Advanced Research core of WRF for the Project Sagebrush phase 1 (PSB1; Finn et al. 2016). The WRF output includes variables required for computing stability parameters, as well as total turbulent kinetic energy and turbulent exchange coefficient so that we can compare and evaluate all mixing options in HYSPLIT with observations taken during the tracer experiment. PSB1 consisted of five tracer releases in the afternoons of October 2013 and aimed for the sub-kilometer scale transport with near neutral or unstable stability conditions. Flux measurements, including turbulent velocity variance, are available along with tracer concentration observations, which provides a platform for the direct evaluation of the turbulent variables and the evaluation of dispersion results corresponding to different mixing options. Prior to this study Ngan et al. (2018) assessed the performance of the WRF-HYSPLIT modeling system for the dispersion scenario represented by PSB1, featuring daytime convective conditions at fine spatial (a few hundred meters) and temporal (10-min averaging) scales. The turbulent mixing is an essential component affecting HYSPLIT's performance but not yet investigated in the previous study. Thus, in the current work, we focus on evaluating the turbulent mixing methods available in HYSPLIT and their impacts on dispersion results as compared against PSB1 which offers a unique set of observations for the comparison of both velocity variance and tracer concentration. In addition, we conducted HYSPLIT simulations driven by the WRF data using different mixing options for the Cross Appalachian Tracer Experiment (CATEX; Ferber et al. 1986). Unlike the Sagebrush experiment focusing on a fine spatial and temporal scale, CAPTEX consisting of six 3-h releases aimed to simulate the long-range transport and diffusion of pollutants. The evaluations of dispersion results with measured concentrations provide the insight to assess the performance of different mixing methods.

The rest of the paper is organized as follows. Section 2 reviews the different options in HYSPLIT to compute the velocity variance. Section 3 describes the model configurations for the meteorological and dispersion models. In Section 4, we evaluated the velocity variance computed in HYSPLIT with measurements taken during the Sagebrush experiments. The dispersion simulations for the controlled tracer experiment – PSB1 and CAPTEX were compared with measured concentration in Sections 5 and 6, respectively. Finally, Section 7 presents the conclusions and future research directions.

2. Overview of mixing options in HYSPLIT

To compute the transport and mixing of particles, HYSPLIT treats the advection and dispersion processes separately. The advection calculation uses the three-dimensional velocity field while the dispersion calculation requires the standard deviations of the turbulent velocity $\{\sigma_i = [\sigma_w, \sigma_u, \sigma_v]\}$ to add a random component to the advective motion. There are different methods to estimate the standard deviation of turbulent velocity based on the availability of stability and turbulent parameters in the meteorological data. The full list of equations for all parameters associated with each method is in Draxler and Hess (1998). An abstract of the four mixing options available in HYSPLIT is described below.

a. Beljaars-Holtslag (BH) method

Following Beljaars and Holtslag (1991) for a stable surface layer, and Betchov and Yaglom (1971) and Kadar and Perepelkin (1989) for an unstable surface layer, the model computes the normalized profiles for heat and momentum, and then the vertical mixing coefficient according to the profiles and other stability parameters such as friction velocity, convective velocity scale, and Obukhov length. To obtain the vertical velocity variance, the model divides the diagnosed mixing coefficient by a Lagrangian time scale. This option is labeled hereafter as “BH”.

b. Kantha-Clayson (KC) method

Following Kantha and Clayson (2000), the model defines the turbulent velocity variances as a function of friction velocity, convective velocity scale, and boundary layer depth. HYSPLIT uses it as the default when the momentum and heat flux variables are available in the meteorological data. This method (named hereafter “KC”) does not need the intermediate step of computing the mixing coefficient and the use of turbulent time scales.

c. Using the turbulent kinetic energy (TKED)

If the meteorological data provide the turbulent kinetic energy, the model partitions the values to the vertical and horizontal components using the anisotropy ratio. According to experimental data, about one-third of TKE are assigned to the vertical velocity variance while twice as much of the values are partitioned to the horizontal components. HYSPLIT uses this as default anisotropy. However, users can let the model compute the anisotropy factors according to the Kantha-Clayson equations instead of using a partitioning factor constant in space and time. This option is labeled hereafter as “TKED”.

d. Using the turbulent exchange coefficient (EXCH)

This method computes the velocity variance by dividing the turbulent exchange coefficient by the vertical Lagrangian time scale, which is set to 100 s following Draxler and Hess (1998). This option is labeled hereafter as “EXCH” and is newly added to HYSPLIT with using the WRF meteorology. The turbulent exchange coefficient is computed within the user-selected planetary boundary layer (PBL) parameterization in WRF. The two classes of PBL approaches are 1.5-order TKE based schemes and first-order diagnostic K-profile schemes. The former diagnoses the exchange coefficient as a function of the mixing length, stability function, and prognostic TKE while the latter computes it from variables such as velocity scale, PBL height, and Prandtl number (Shin and Dudhia, 2016).

3. Experimental Data and Model Configurations

The Project Sagebrush phase 1 tracer fields experiment took place at the Idaho National Laboratory (43.59 N and 112.94 W) during October 2013 to understand sub-kilometer dispersion by performing continuous 2.5-h inert tracer (SF_6) releases over flat terrain (Finn et al. 2016). Tracer releases were conducted on five afternoons (intensive observation periods, or IOPs) under either neutral or unstable stability conditions. The measurement network consisted of five concentric arcs located from 200 – 3200 m away from the release location. Tracer samples were obtained starting 30 minutes after the release in 10-min intervals. Comprehensive meteorological measurements, including turbulent velocity variance data, were available during the experimental period.

The WRF Version 3.7 was used to generate meteorological data for the controlled tracer experiments. The domain configuration and physic options followed Ngan et al. (2018) for PSB1. In this study, we selected the Mellor-Yamada-Nakanishi-Niino (MYNN) 2.5 level TKE scheme (Nakanishi and Niino, 2006) for the planetary boundary layer (PBL) parameterization and the corresponding MYNN surface layer scheme which works together with the Noah land surface model (Chen and Dudhia, 2001) as lower boundary conditions to provide the surface forcing for the vertical transport (Shin et al. 2012). The evaluations in Ngan et al. (2018) showed that the meteorological data for IOP4 and IOP5 featuring unstable conditions with moderate winds were simulated well by WRF. However, the model performance was degraded due to the underestimation of strong winds in IOP3 with neutral conditions and the inaccurate prediction of wind direction in IOP2 featuring unstable conditions with light winds. This study did not include IOP1 due to the sampling network not observing the plume (Finn et al. 2015). HYSPLIT simulations were configured following Ngan et al. (2018); 250,000 Lagrangian particles were released and lasted two-and-a-half hours. The tracer concentration was calculated by summing particles in the volume of 100 x 100 m and from the surface to 25 m above ground. Time averaging was set to 10 minutes. HYSPLIT was driven by WRF model output with a horizontal resolution of 0.333-km (the most inner WRF domain) and a temporal resolution of 5 minutes. A sensitivity test on the meteorological grid and its impact on the dispersion results for tracer releases in PSB1 was presented in Ngan et al. (2018). The analysis shows that under the meteorological conditions represented by PSB1, the HYSPLIT results for IOP 2, 4, and 5 were not sensitive to the grid resolution of the

WRF data. The mixing options described in Section 2 were used to simulate four IOPs conducted in PSB1.

CAPTEX took place in the northeastern United State and southeastern Canada from mid-September through the end of October 1983. An inert perfluorocarbon tracer were released to simulate the transport and dispersion of pollutants at scales of hundred to a thousand kilometers (Ferber et al. 1986). Six 3-h releases were conducted at Dayton, Ohio during the afternoon (releases 1-4) and at Sudbury, Ontario, Canada during the nighttime (releases 5 and 7). The measurement network included 85 ground-level stations distributed 300 – 800 km from the source, providing 3- and 6-h average tracer concentrations for three-day periods after the tracer release. WRF data with a horizontal resolution of 9 km was the meteorological input to drive HYSPLIT. The WRF simulation was initialized by the WRF archived dataset and nested in the coarse resolution domain introduced in Ngan and Stein (2017). The simulation used the MYNN 2.5 level TKE-based PBL scheme and its corresponding surface layer scheme, while other physics options followed Ngan and Stein (2017). The hourly meteorological files were used to drive HYSPLIT simulations running with the four mixing options. A concentration grid with ~25-km horizontal resolution was set for the simulations with one vertical layer from 0 – 100 m above ground. Detailed information of each release is described in Ngan and Stein (2017).

4. Comparisons of the velocity variances

Figure 1 is the layout of the sampling arcs for the tracer concentration and the meteorological observation taken during PSB1. The velocity variance (or the standard deviation of velocity) was measured at six locations and different heights (Table 1) with two sodars at the ASC and ART stations, and 3-d sonic anemometers at the other velocity variance sites (Finn et al. 2016). The measurement of TKE by the ASC site tended to match well to the measurement of TKE by the five other sites using the 3-d sonic anemometer while the TKE measurement at the ART site was an order of magnitude higher than the others. Note that the vertical turbulence measurements at these two sodar sites are roughly similar in magnitude much of the time. The difference between two sodars for the observed TKE arises from the measurements along the u and v beams (Finn et al. 2015). Thus, we excluded the ART sodar results that are probably not reliable for the model comparison. This section discusses the velocity variance estimated by different mixing options in HYSPLIT and shows the evaluations with observations taken during PSB1.

a. Comparisons of the vertical velocity variances

The vertical velocity variance determines how the particles released at the source location are dispersed in space and time. Figure 2 (a – d) is the profile of the vertical velocity variance from HYSPLIT using four different mixing options during 12 – 15 MST on October 5th, 2013 (IOP2). Both BH and KC methods diagnose the vertical velocity variance based upon state variables and variables relevant to the PBL stability. Depending on the stability regimes and the altitudes (within the surface layer, in the PBL, or in the free atmosphere), the model has a different set of equations to diagnose the mixing of particles (Draxler and Hess, 1998). Other than the maximum at the middle of PBL, the profile of BH and KC mixing options had a secondary maximum transitioning from the top of the PBL to the free atmosphere (Figure 2 a and b). The vertical velocity variance profile from the KC option had a small peak within the surface layer while the one from the BH option went to almost zero values near the surface. As shown in Figure 2 c and d, the vertical velocity variance profiles from TKED and EXCH options looked quite different. These two methods depend on the profile of TKE and exchange coefficient provided by WRF, respectively. The definition of TKE is the summation of velocity variances (horizontal and vertical) divided by two that represents the strength of turbulence in the flow. It is computed in WRF's PBL schemes (the MYNN schemes in this study) using the prognostic TKE equation. The turbulent exchange coefficient is a scalar to relate the turbulent flux to the gradient of the associated mean variable. The MYNN PBL scheme diagnoses the exchange coefficient according to the prognostic TKE, a mixing length, and a stability function (Nakanishi and Niino, 2006).

There are studies, such as Munoz-Esparza et al. (2018), Ferrero et al. (2018), and Hari Prasad et al. (2017), showing the problem of the TKE estimation produced by various WRF's TKE-based PBL schemes. Ferrero et al. (2018) evaluated several PBL parameterizations available in WRF with experimental data conducted in Turin, Italy. The results showed the underestimation of the model TKE in comparison with the measurements (anemometer at 25 m height) in a summer month and less underestimation of TKE in a winter month. We compared the predicted TKE from WRF with observed TKE taken at 30 m height of the GRI tower during PSB1. In addition to the MYNN run, other simulations were conducted with different TKE-based PBL schemes, including the Bougeault and Lacarrere scheme (BouLac; Bougeault and Lacarrere, 1989), the Quasi-Normal Scale Elimination scheme (QNSE; Pergaud et al. 2009), the UW boundary layer scheme (UW; Bretherton and Park 2009), the Mellor-Yamada-Janjic (MYJ; Janjic, 1994), and the Grenier-Bretherton-McCaa (GBM; Grenier and Bretherton 2001). The comparison showed all modeled TKE values were underestimated (Figure 3). Among various PBL schemes, the BouLac underpredicted the least and MYNN was the second least underprediction of TKE. The run using MYJ and QNSE schemes underpredicted the most. The length scales and TKE prediction cause the differences in turbulent exchange coefficient computed by various PBL schemes. Among the six schemes, the GMB and UW schemes produced larger exchange coefficient while the QNSE and BouLac had smaller values during PSB1 (not shown). Thus, these meteorological uncertainties may have impact on the dispersion result when we use TKED and EXCH mixing options to estimate the turbulent velocity variance.

The observational tower at the ASC station provides vertical profiles of velocity variance from 30 – 150 m. Observed vertical velocity variance at ASC ranges from 0.2 – 0.9 m^2s^{-2} with the maximum at about 100 m height (Figure 2e). Note that the stability condition on the day of IOP2 was unstable with low wind speeds. The KC and EXCH option generated a maximum vertical velocity variance of about 1.5 m^2s^{-2} at an altitude of about 500 m. The TKED profile had the smallest maximum values (about 0.5 m^2s^{-2}) among all and a smooth decrease with height from a maximum value to a minimum value in the free atmosphere. In the BH case, the vertical velocity variance profile at about 100 m height was similar to the observations but the maximum value was slightly underestimated. Figure 4 is the vertical velocity variance profiles for IOP5 (12 – 15 MST on October 18th, 2013), which was a weakly unstable condition with moderate wind speeds. The modeled vertical velocity variance had less variation throughout the afternoon than the observed values. In comparison with other options, the EXCH profile showed larger temporal variability. Note that the sodar measurements for the turbulent velocity variance available in PSB1 were limited to 30 – 150 m height. The study of Berg et al. (2017) using year-long vertical variance data from Doppler Lidar data for the convective boundary layer showed that the maximum of the composite vertical velocity variance was about 1.2 m^2s^{-2} at about 200 – 700 m height. Thus, the velocity variance measurements from PSB1 were insufficient to evaluate the simulated maximum vertical velocity variance, which might occur at the altitude above the sodar could reach.

The comparison of vertical velocity variance at and below 30 m was done using measurements of 3-d sonic anemometers at the FLX station (3.2 m; Figure 5) and the GRI station (30 m; Figure 6). The magnitude of the observed vertical velocity variance in the afternoons of four IOPs was about 0.2 m^2s^{-2} near the surface (3.2 m height). IOP 3 was an exception that its value went up to 0.6 m^2s^{-2}. As discussed in Finn et al. (2015), tracer releases in PSB1 were conducted on days with unstable (or weakly unstable) stability conditions but IOP3 experienced a neutral condition with strong wind speeds. The meteorological evaluation presented in Ngan et al. (2018) showed that WRF failed to generate the rapid increase of high wind speeds observed during IOP3 causing negative bias for the friction velocity. Thus, we expected the KC option would underestimate the turbulent mixing because the velocity variances were diagnosed as a function of friction velocity. In general, the KC and TKED mixing methods overestimated the vertical velocity variance (except IOP3) while the EXCH mixing slightly underestimated it. At 30 m height (GRI station), the observed vertical velocity variance was about 0.4 – 0.6 m^2s^{-2}. The KC, TKED, and EXCH options generated the values comparable to the measurements while the vertical velocity variance from KC was larger than those from other mixing options. The vertical velocity variance generated by the BH method was underestimated the most in the comparison with measurements at both 3.2 m and 30 m.

b. Estimation of the horizontal velocity variances

The mixing methods determine the way the meteorological data are processed to compute vertical and horizontal turbulence. In this study, the horizontal velocity variance was obtained in proportion to the vertical component. Figure 7 is the time series of horizontal velocity variance at the FLX station. The magnitude was about 1.2 – 1.8 m^2s^{-2} in the afternoon during the period of tracer release. For the BH mixing scheme, the diagnosed turbulence is portioned equally between the vertical and horizontal component resulting in a larger negative bias in the horizontal velocity variance. For the KC and TKED mixing options, the calculation has more turbulence going into the horizontal component than the BH method does (Stein et al. 2015). The horizontal velocity variance in KC and TKED mixing were comparable to the measured values with a small underestimation. The underestimations of horizontal velocity variances were more significant in IOP3 than other episodes because of the under-prediction of the wind fields and vertical mixing.

Using velocity variance measurements taken at different locations and heights in the area of the sampling array, we computed the ratio of the horizontal and vertical components (Table 1). The right-most column of the table includes the data only in the afternoon of four IOP days. The ratio was in the range of 4.5 – 5.8 for data measured near the surface at 3.2 m or 4 m height. It became smaller, ranging about 1.5 – 2.6, when using data observed at higher levels (30 m or 45 m). The sodar measurement at the ASC station showed the ratio of horizontal and vertical velocity variance got to about a one to one ratio at 130 m. For the EXCH mixing option, we selected the maximum (5.8733) and minimum value (1.5430) of the ratios at near surface and 45 m height, respectively. They were applied to compute the horizontal velocity variance. Two cases, labeled as "EXCH" and "EXCHm" using the maximum and minimum ratios, respectively, were included in Figure 7. With a larger scaling factor, EXCH had a larger horizontal velocity variance than EXCHm which used a smaller scaling factor. However, both cases underestimated horizontal velocity variance in comparison with the measurements at 3.2 m height. For the comparison with data at 30 m height, the underestimation decreased.

5. Dispersion results for PSB1

We conducted HYSPLIT simulations performed with different turbulent mixing parameterizations and driven by WRF meteorological model output for the four IOPs from PSB1. The mixing options described in the previous section were labeled as BH, KC, TKED and EXCH. For the mixing option using WRF's turbulent exchange coefficient, we conducted two simulations "EXCH" and "EXCHm" by applying the maximum and minimum ratio of the horizontal and vertical component of measured velocity variance. The statistical evaluation followed Draxler (2006) which introduced a cumulative score (so called the Rank, ranging from 0 to 4) including four normalized components – the correlation coefficient (R), fractional bias (FB), figure-of-merit in space (FMS), and Kolmogorov-Smirnov parameter (KSP).

$$Rank = R^2 + 1 - \left|\frac{FB}{2}\right| + \frac{FMS}{100} + \left(1 - \frac{KSP}{100}\right)$$

Figure 8 shows the statistical rank of five dispersion simulations for each IOP in PSB1. The model performed differently with varying mixing options for different episodes, but no one mixing option always produced a better result. In general, the range of statistical scores of simulations using different mixing options for IOP4 and IOP5 was smaller than those for the other two IOPs, possibly due to WRF more accurately simulating the wind patterns during IOP4 and IOP5 than IOP2 and IOP3. Other than the dispersion process in which the estimation of turbulent velocity variance is an essential component, the advection process driven by the mean winds determines the movement of the tracer plume. In the IOP4 and IOP5 scenarios, the tracer plume was transported by northwesterly flows steadily from the source toward the outer arcs of the sampling array and without much variation throughout the release duration. In general, the rank for EXCH was better than EXCHm for all four episodes because the larger horizontal velocity variance in the EXCH simulation generated a wider plume. However, the dispersion result was not very sensitive to the horizontal velocity variance since the wind shear was the dominant factor for the spreading of the plume in the horizontal direction.

IOP2 had the lowest rank among all four episodes due to the inaccurate prediction of varying wind directions associated with the light winds. The modeled plume was narrower and further downwind, going northeastward to the outer arcs of the sampling array, than the observed plume (Figure 9). In this case, the strong mixing produced by the KC and EXCH method was able to disperse particles more, which resulted in less overestimation (smaller FB in the rank bar-chart) of the tracer concentration compared to other cases. We notice the underprediction of TKE in the comparison of the observed values at the ASC station (not shown) that caused the weak mixing in the TKED method. A sensitivity test was conducted using two times of TKE values from WRF to drive a dispersion simulation with the TKED mixing option. This result had better statistical scores (Rank=1.67) compared to the result shown in Figure 9 (Rank=1.47) because the stronger mixing was able to improve the overprediction of the surface concentration and the coverage of the plume.

For IOP3, even though the rank had better statistical scores than IOP2, the simulated plume went out of the sampling array at the beginning of the release. The weaker mixing generated by the BH and TKED method resulted in higher concentrations near the source location (better FB in the rank bar-chart) than EXCH did. However, the BH plume was narrow due to the significant underestimation of the horizontal velocity variance that resulted in getting the worst rank. For the scenario of IOP3, the strong mixing in the EXCH simulation caused more underprediction of surface concentration (worse FB) than other cases. Compared to the TKED plume (Figure 10d), the EXCH plume had a lower concentration and was slightly wider. The surface wind measurements indicated strong southwesterly winds during the tracer release while WRF generated light wind speeds and varying wind directions until southwesterly winds picked up during the second hour of the release (Ngan et al. 2018). The underestimation of the turbulence near the surface in the KC mixing option (referring to Figure 5 and Figure 6) due to the negative bias in the wind speed and friction velocity might cause less mixing than others. As shown in the difference plot (Figure 10c), the KC case had more particles accumulating near the source location (in the area within the 200-m arc) while the TKED run moved particles farther away.

6. Dispersion results for CAPTEX

HYSPLIT simulations driven by WRF with 9-km grid spacing were conducted using the four mixing options for the six releases during CAPTEX. Figure 11 shows the time series of vertical velocity variance profiles for 24 hours after the beginning of an afternoon tracer release at Dayton, Ohio (CAPTEX 1). The KC and EXCH mixing had the maximum vertical velocity variance at the 10th model layer (~900 m) during the afternoon hours (17 – 21 UTC). The maximum values were smaller and occurred at the lower layers in the other two mixing methods. The profile of the vertical velocity variance generated by the TKED method was flat with values ranging from about 1.0 – 1.4 m^2s^{-2} from the surface to the middle of the PBL where the maximum was observed. However, the profile in the EXCH mixing option had large gradients near the surface (the lowest 3 model layers, 0 – 70 m) and at the top of PBL (13^{th} – 15^{th} model layer, 1.5 – 2.0 km). During the nighttime, close to zero vertical velocity variance values were produced by the EXCH mixing. This is due to a constant Lagrangian time scale that was used for the daytime unstable condition. Unlike PSB1 episodes that all occurred in the afternoon with well-mixed conditions, for scenarios like CAPTEX experiencing different stability conditions throughout the day, a time-varying Lagrangain time scale will be more appropriate for estimating the turbulent velocity variance. Figure 12 is an example of CAPTEX 7, which was a nighttime release at Sudbury, Ontario, Canada. Similar patterns for the vertical velocity variance profile were observed in other releases of CAPTEX.

The BH and KC simulations had similar horizontal and vertical distribution patterns of particles for CAPTEX 1 and resulted in comparable statistical ranks (Figure 13). There were more particles moved to upper levels and less particles stayed in the lowest 500 m in the TKED simulation. In general, particles were mixed to higher altitudes in the TKED option since its vertical velocity variance profile extended to higher levels than others. In the EXCH case, particles near the surface (the lowest 500 m) moved slower than the particles above. That may be due to the almost zero vertical mixing during the nighttime, resulting in particles remaining over Lake Erie and Lake Ontario and positive bias of tracer concentration in those area. For CAPTEX 7, the 48-hour averaged concentration patterns generated by the KC and TEKD mixing were similar as shown in Figure 14. The tracer plume in EXCH was narrow at the beginning of the episode and then became wider in the downwind area that resulted in worse statistical scores than other simulations. The constant turbulent time scale used in the EXCH option for computing vertical velocity variances might cause too little mixing at night and overestimation during daytime. Overall, the statistical rank for all six CAPTEX episodes (Table 2) shows that the TKED mixing had good performance while the BH options produced the worst results. For individual episodes, except CAPTEX 2 in which all four mixing options performed similarly, there was no one scheme that always outperforms the other options. It is appropriate to keep various options for users to choose depending on different scenarios or to create dispersion ensembles.

7. Summary and discussion

The turbulent velocity variance is an essential variable in HYSPLIT to determine the mixing of particles. There are different options available in the model to estimate the turbulent velocity variance according to the stability and turbulent variables provided by the meteorological data. In this study, we conducted HYSPLIT simulations driven by WRF meteorology and using different mixing methods for two control tracer experiments – PSB1 and CAPTEX that aimed for the sub-kilometer and long-range transport, respectively. Through the comparisons of turbulent velocity variance (only for PSB1) and the evaluation of tracer concentrations with measurements, we assessed the performance of different mixing options affecting the dispersion results.

The KC and EXCH mixing options produced a larger maximum of the vertical velocity variance than other mixing options did. Simulated maximum vertical velocity variance occurred at an altitude of about 500 m, which is above the tower measurement available in the PSB1. The vertical velocity variance profile obtained from the BH method had a sharp increase from the surface to the height of the maximum values (about 200 m). The TKED case had a flat vertical velocity variance profile with the smallest variation in its value with height and maximum compared to other cases. The comparison with measurements near the surface (height at 3.2 m and 30 m) taken during the PSB1 showed that the BH scheme underestimated vertical velocity variance while the KC option slightly overestimated it. The dispersion results for IOP4 and IOP5 (weak unstable conditions with moderate winds) were less sensitive to the mixing option than the runs for IOP2 (unstable with light winds) and IOP3 (neutral with strong winds). The plumes generated by the BH and TKED method (less disperse due to the weaker vertical velocity variance) had higher concentrations near the surface than those driven by the KC and EXCH option (stronger mixing). The larger horizontal velocity variance in the EXCH generated a slightly wider plume than the one in the EXCHm simulation. HYSPLIT simulations using different mixing options were conducted for six CAPTEX episodes. The statistical rank for the TKED run was slightly better than others while the BH mixing generated results with the worst rank. For scenarios like CAPTEX experiencing different stability conditions throughout the day, a time-varying Lagrangain time scale may be more appropriate for estimating the turbulent velocity variance.

The model performed differently with the four mixing options in varying scenarios. No one mixing option always outperformed the other options. HYSPLIT users can select a mixing option according to their scenario and availability of meteorological fields, as well as use different mixing options to generate dispersion ensembles. The KC and BH methods re-compute various stability parameters with assumptions for different stability conditions to obtain the turbulent velocity variance for the dispersion process. Errors due to the process of re-diagnosing variables may be carried to the dispersion simulation. However, the advantage of these two methods is that unlike the other options, no extra variable is required. If only basic meteorological parameters such as wind, temperature, and pressure are available, HYSPLIT has an alternative option to estimate the boundary layer stability parameters for computing the turbulent velocity variance (Stein et al. 2015).

The TKED and EXCH options depend on the mixing variables (TKE and exchange coefficient, respectively) provided by WRF. If the meteorological data provide well-simulated TKE fields, HYSPLIT can obtain the velocity variance by partitioning the horizontal and vertical components. Thus, the main concern for HYSPLIT is to set a reasonable anisotropy ratio. Note that there is no TKE output if a first-order K-profile PBL scheme is used for running the meteorological simulation. The underestimation of TKE values by WRF in the unstable condition shown in the comparison with measurements from PSB1 needs further investigation. For the EXCH option, the turbulent exchange coefficient is needed, but it is not commonly available in meteorological model output or reanalysis products that can be used to drive HYSPLIT. Different PBL schemes have their ways of computing the exchange coefficient, and the results are rarely evaluated. It is recommended to use a time-varying Lagrangian time scale to estimate the velocity variance with the turbulent exchange coefficient. The uncertainty of TKE and exchange coefficient prediction may influence the dispersion simulation when the velocity variance is computed by the TKED or EXCH mixing option. For future works, we are interested in an evaluation of modeled vertical velocity variance with long-term observations that may further give us insight how each mixing option performs for stable nighttime conditions and unstable daytime conditions. Such measurements may be found in the DCNet research network (Hicks et al. 2013) and Doppler Lidar data (Berg et al. 2017). The DCNet data are measurements at six suburban areas in the eastern United States while Lidar measurements can provide data covering the entire PBL. With continuous measurements, the velocity variance evaluation is not limited to certain days or stability scenarios. Furthermore, Project Sagebrush Phase 2 (PSB2; Finn et al. 2018), which was conducted in 2016, consisted of four IOPs during very unstable conditions and four IOPs during very stable conditions. Similar to the setup of PSB1, velocity variance observations are available along with tracer concentration measurements that can be used to evaluate HYSPLIT's turbulent mixing options and their impact on dispersion results.

Acknowledgements

This study was supported by NOAA grant NA14NES4320003 (Cooperative Institute for Climate and Satellites -CICS) at the University of Maryland/ESSIC.

References

Beljaars, A.C.M., and A.A.M. Holtslag, 1991: Flux parameterizations over land surfaces for atmospheric models. *J. Appl. Meteorol.*, **30**, 327-341.

Berg L. K., R. K. Newsom, and D. D. Turner, 2017: Year-long vertical velocity statistics derived from Doppler Lider data fro the continental convective boundary layer. *J. Appl. Meteorol. Clim.*, **56**, 2441-2454.

Betchov, R., and A.M. Yaglom, 1971: Commetns on the theory of similarity as applied to turbulence in an unstably stratified fluid. *Atmos. Oceanic Phys.,* **7,** 829-832.

Bougeault, P., and P. Lacarrere, 1989. Parameterization of orography-induced turbulence in a mesobeta-scale model. *Mon. Weather Rev.*, **117**, 1872–1890.

Bretherton, C. S., and S. Park, 2009: A New moist turbulence parameterization in the Community Atmosphere Model. *J. Climate*, **22**, 3422–3448, doi:10.1175/2008JCLI2556.1.

Kantha, L.H. and C.A. Clayson, 2000: Small Scale Processes in Geophysical Fluid Flows, Vol. 67, International Geophysics Series, Academic Press, San Diego, CA, 883 pp.

Kadar, B.A., and V.G. Perepelkin, 1989: Effect of the unstable stratification on wind and temperature profiles in the surface layer. *Atmos. Oceanic Phys.,* **25,** 583-588.

Chen, F., and J. Dudhia, 2001: Coupling and advanced land surface–hydrology model with the Penn State–NCAR MM5 modeling system. Part I: Model implementation and sensitivity. *Mon. Wea.Rev.*, **129**, 569–585.

Dee, D. P. and Co-authors, 2011: The ERA-Interim reanalysis: configuration and performance of the data assimilation system. *Quarterly Journal of the Royal Meteorol. Soc.,* **137**, 553-597.

Draxler, R. R., 2006: The use of global and mesoscale meteorological model data to predict the transport and dispersion of tracer plumes over Washington, D.C. *Wea. Forecasting*, **21**, 383–394.

Draxler, R. R. and G. D. Hess, 1997: Description of the HYSPLIT_4 modeling system. NOAA Tech. Memo. ERL ARL-224, NOAA/Air Resources Laboratory, Silver Spring, MD, 24 pp. [Available online at http://www.arl.noaa.gov/documents/reports/arl-224.pdf.]

Draxler, R. R. and G. D. Hess, 1998: An overview of the HYSPLIT_4 modeling system for trajectories, dispersion, and deposition. *Aust. Meteor. Mag.*, **47**, 295–308.

Ferber, G. J., J. L. Heffter, R. R. Draxler, R. J. Lagomarsino, F. L. Thomas, and R. N. Dietz, 1986: Cross-Appalachian Tracer Experiment (CAPTEX-83) final report. NOAA Tech. Memo. ERL ARL-142, 60 pp. [Available online at http://www.arl.noaa.gov/documents/reports/arl-142.pdf]

Ferrero, E., S. Alessandrini, and F. Vandenberghe, 2018: Assessment of Planetary-Boundary-Layer schemes in the Weather Research and Forecasting model within and above an urban canopy layer. *Bound.-Layer Meteor.*, **168**, 289–319.

Finn, D., K .L. Clawson, R. M. Eckman, H. Liu, E. S. Russell, Z. Gao, and S. Brooks, 2016: Project Sagebrush: Revisiting the value of the horizontal plume spread parameter σy. *J. Appl. Meteorol. Clim.*, **55(6)**, 1305-1322. doi: 10.1175/JAMC-D-15-0283.1

Finn, D. and Coauthor, 2015: Project Sagebrush Phase 1. NOAA Tech Memo OAR ARL-268, 362 pp. [Available online at https://www.arl.noaa.gov/documents/reports/ARL-TM-268.pdf]

Finn, D., R. G. Carter, R. M. Eckman, J. D. Rich, Z. Gao, and H. Liu, 2018: Plume Dispersion in Low-Wind-Speed conditions during Project Sagebrush Phase 2, with emphasis on concentration variability. *Bound.-Layer Meteor.*, **169**, 67–91.

Grenier, H., Bretherton, C.S., 2001. A moist PBL parameterization for large-scale models and its application to subtropical cloud-topped marine boundary layers. *Mon. Weather Rev.*, **129**, 357–377.

Hari Prasad, K. B. R. R., C. V. Srinivas, T. Narayana Rao, C. V. Naidu, R. Baskaran, 2017: Performance of WRF in simulating terrain included flows and atmospheric boundary layer characteristics over the tropical station Gadanki. *Atmospheric Research*, **185**, 101-117.

Hicks, B. B., E. Novakovskaia, R. J. Dobosy, W. R. Pendergrass, and W. J. Callahan, 2013: Temporal and spatial aspects of velocity variance in the urban surface roughness layer. *J. Appl. Meteor. Climatol.*, **52**, 668-681.

Janjic, Z.I., 1994: The step-mountain eta coordinate model: further developments of the convection, viscous sublayer, and turbulence closure schemes. *Mon. Weather Rev.*, **122**, 927–945.

Kanamitsu, M., 1989: Description of the NMC global data assimilation and forecast system. *Weather Forecast*, **4**, 334–342.

Munoz-Esparza, D., R. D. Sharman, and J. K. Lundquist, 2018: Turbulence Dissipation Rate in the Atmospheric Boundary Layer: Observations and WRF Mesoscale Modeling during the XPIA Field Campaign. *Mon. Weather Rev.*, **146,** 351-370.

Nakanishi, M. and H. Niino, 2006: An Improved Mellor–Yamada Level-3 Model: Its Numerical Stability and Application to a Regional Prediction of Advection Fog. *Bound.-Layer Meteor.*, **119**, 397-407.

Ngan, F. and A. Stein, 2017: A Long-Term WRF Meteorological Archive for Dispersion Simulations: Application to Controlled Tracer Experiments, *J. Appl. Meteor. Climatol.*, **56**, 2203–2220, https://doi.org/10.1175/JAMC-D-16-0345.1

Ngan, F., A. Stein, D. Finn, and R. Eckman, 2018: Dispersion Simulations using HYSPLIT for the Sagebrush Tracer Experiment. *Atm. Environ.*, **186**, 18-31.

Pergaud, J., Masson, V., Malardel, and S., Couvreux, F., 2009. A parameterization of dry thermals and shallow cumuli for mesoscale numerical weather prediction. *Bound.-Layer Meteor.*, **132**, 83–106.

Powers, J. G. and Co-authors, 2017: The Weather Research and Forecasting Model: Overview, System Efforts, and Future Directions. *Bull. Amer. Meteor. Soc.,* **98**:8, 1717-1737.

Rienecker, M. M. and Co-authors, 2011: MERRA: NASA's Modern-Era Retrospective Analysis for Research and Applications. *Journal of Climate.*, **24**, 3624-3648.

Shin, H. H., S. Y. Hong and J. Dudhia, 2012: Impacts of the Lowest Model Level Height on the Performance of Planetary Boundary Layer Parameterizations. *Mon. Wea. Rev.*, **140**, 665-682.

Shin, H. H. and J. Dudhia, 2016: Evaluation of PBL Parameterizations in WRF at Subkilometer Grid Spacings: Turbulence Statistics in the Dry Convective Boundary Layer. *Mon. Wea. Rev.,* **144**, 1161-1177.

Stein, A. F., R. R. Draxler, G. D. Rolph, B. J. B. Stunder, M. D. Cohen and F. Ngan, 2015: NOAA's HYSPLIT atmospheric transport and dispersion modeling system. *Bull. Amer. Meteor. Soc.*, **96**, 2059-2077.

List of Tables

List of Figures

Figure 13 Horizontal and vertical distribution of particles simulated by HYSPLIT using different mixing options at September 19^{th} 06 UTC, 1983 (CAPTEX 1). Colors indicate particles at different altitudes. Rank of each simulation is noted in each panel.
Figure 14 Tracer concentration plots for CAPTEX 7 from HYSPLIT simulations using different mixing options. The shaded color is 48-hour averaged model concentrations while color-coded circles are measured concentrations. Rank of each simulation is noted in each panel. Unit: log(pg/m^{-3}).

Table 1 The ratio of u- and w-variance computed by using measurements taken during the Sagebrush experiment.

Station name	Measurement Height (m)	All data in October	Data on the day of IOPs	Data during 12-18MST on IOP days
G1	4	3.7041	4.1874	4.5567
G2	30	2.4748	2.6607	2.6127
R1	45	1.8743	1.8830	1.9990
R2	3.2	4.2582	4.5396	4.5487
R3	3.2	4.4776	5.1804	5.3276
R4	3.2	4.6456	5.6300	5.8733
FLX	3.2	3.9803	4.6829	5.3066
ASC	30	-	1.5909	1.8236
	40	-	1.4331	1.5430
	50	-	1.4335	1.4650
	60	-	1.3115	1.3045
	70	-	1.1898	1.2175
	80	-	1.1499	1.1052
	100		1.0902	1.0343
	130	-	1.0646	1.0058
	160	-	1.1152	0.8208

Table 2 Rank corresponding to HYSPLIT model results for six CAPTEX tracer releases.

Release	BH	KC	TKED	EXCH
R1	2.49	2.50	2.62	2.38
R2	2.78	2.72	2.73	2.79
R3	1.98	1.95	2.11	2.13
R4	2.14	2.18	2.16	2.49
R5	2.64	2.52	2.65	2.68
R7	2.25	2.36	2.33	2.12
All[a]	2.35	2.49	2.51	2.44

[a] All data points from six releases are used.

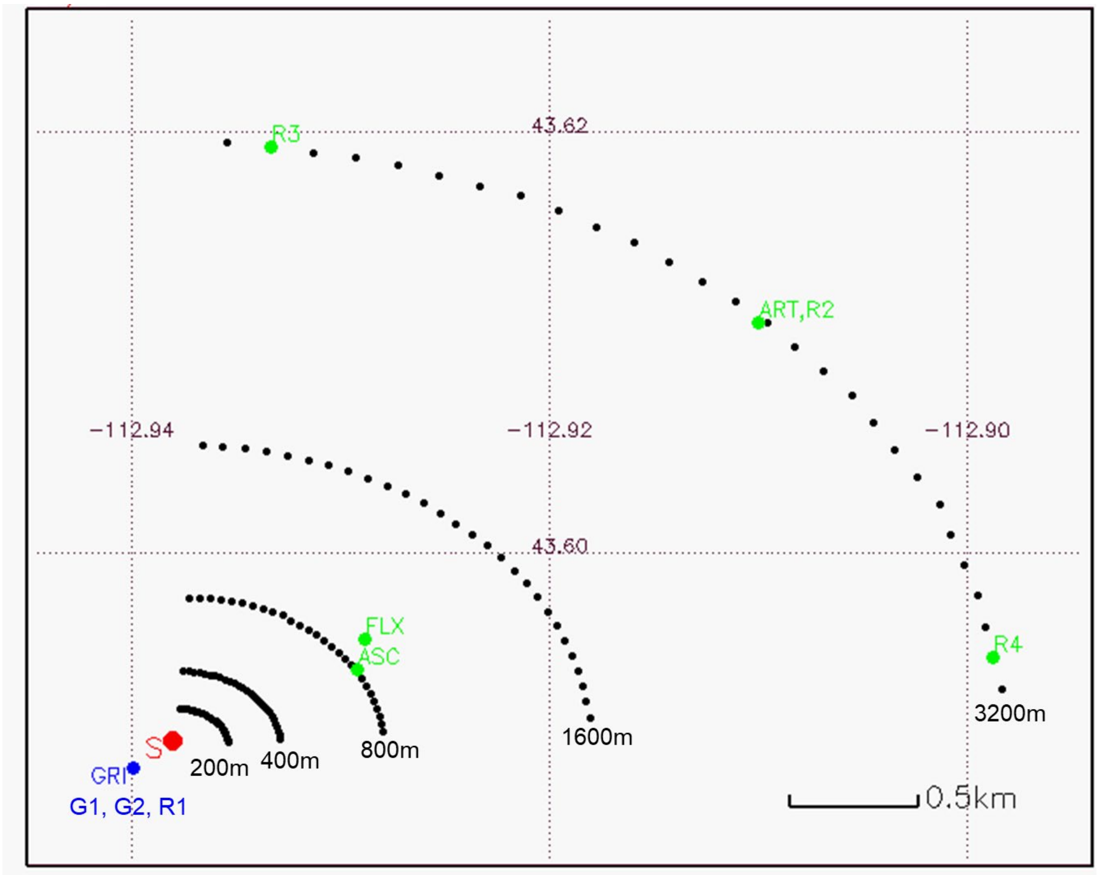

Figure 1 Sampling network for tracer measurements (black dots) for the Sagebrush tracer experiment. The red dot (labeled "S") is the release location of tracer. The measurements for velocity variance were taken at stations labeled as GRI, FLX, R2, R3, and R4 while the measurements for standard deviation of velocity were taken at stations labeled as ASC and ART.

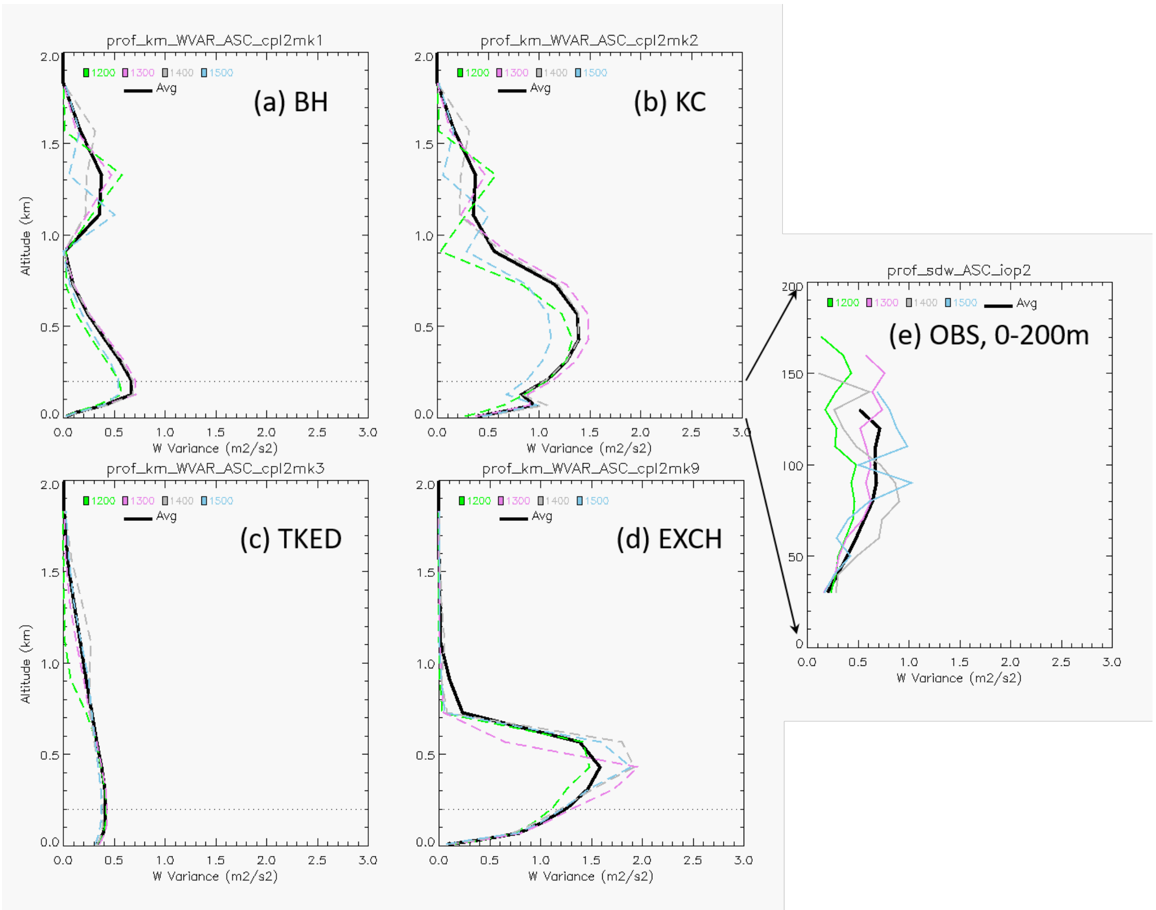

Figure 2 The vertical profile of vertical velocity variance computed using different mixing options in HYSPLIT (a-d) and from the measurement taken at the ASC station (e). Color-code lines indicate different hours during the IOP 2. The black lines are the averaged vertical velocity variance for 12 – 15 MST on October 5th, 2013.

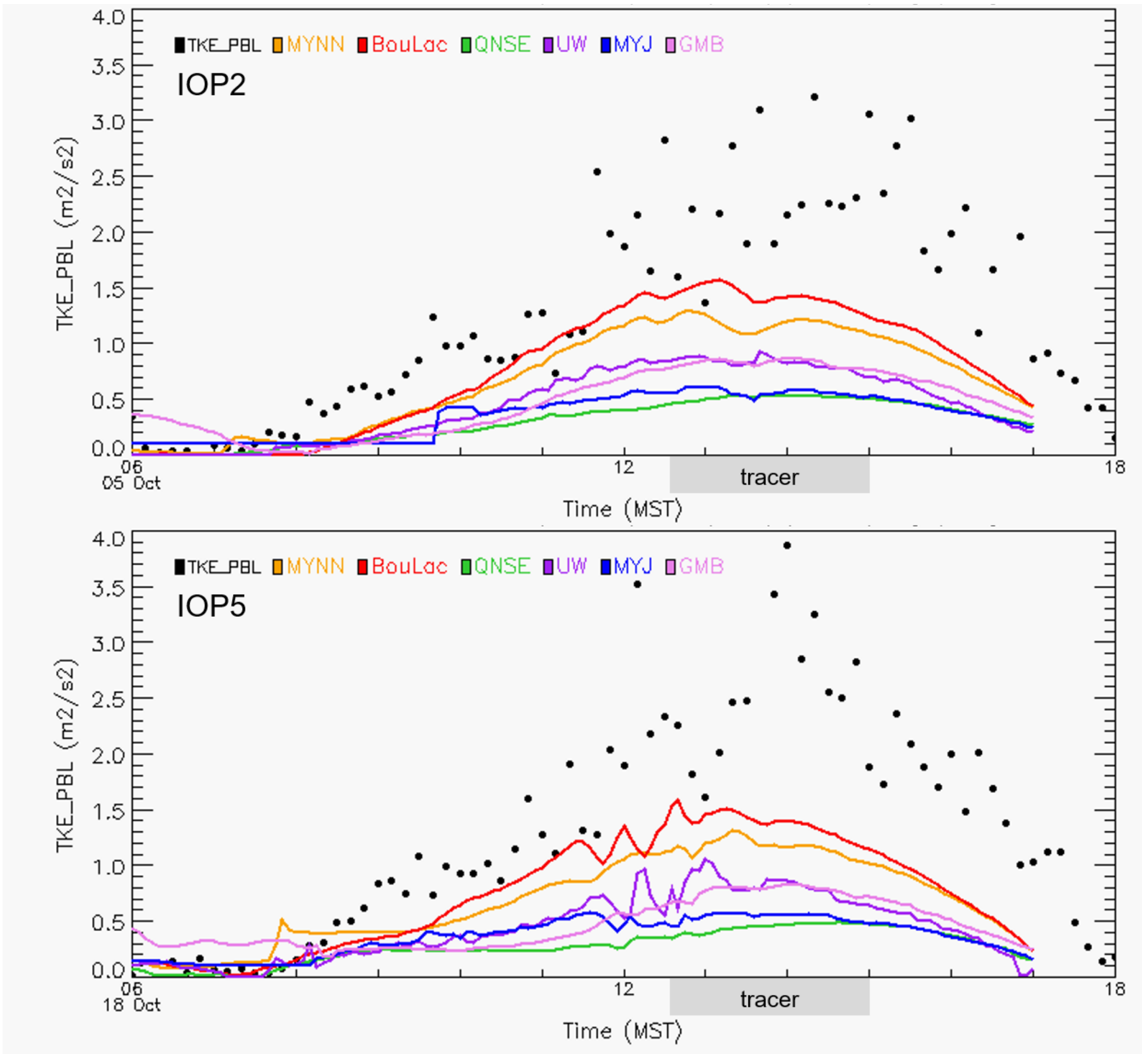

Figure 3 The time series of observed and modeled TKE (m^2s^{-2}) at the GRI tower (30 m height) for IOP2 and IOP5 from WRF simulations using different TKE-based PBL schemes.

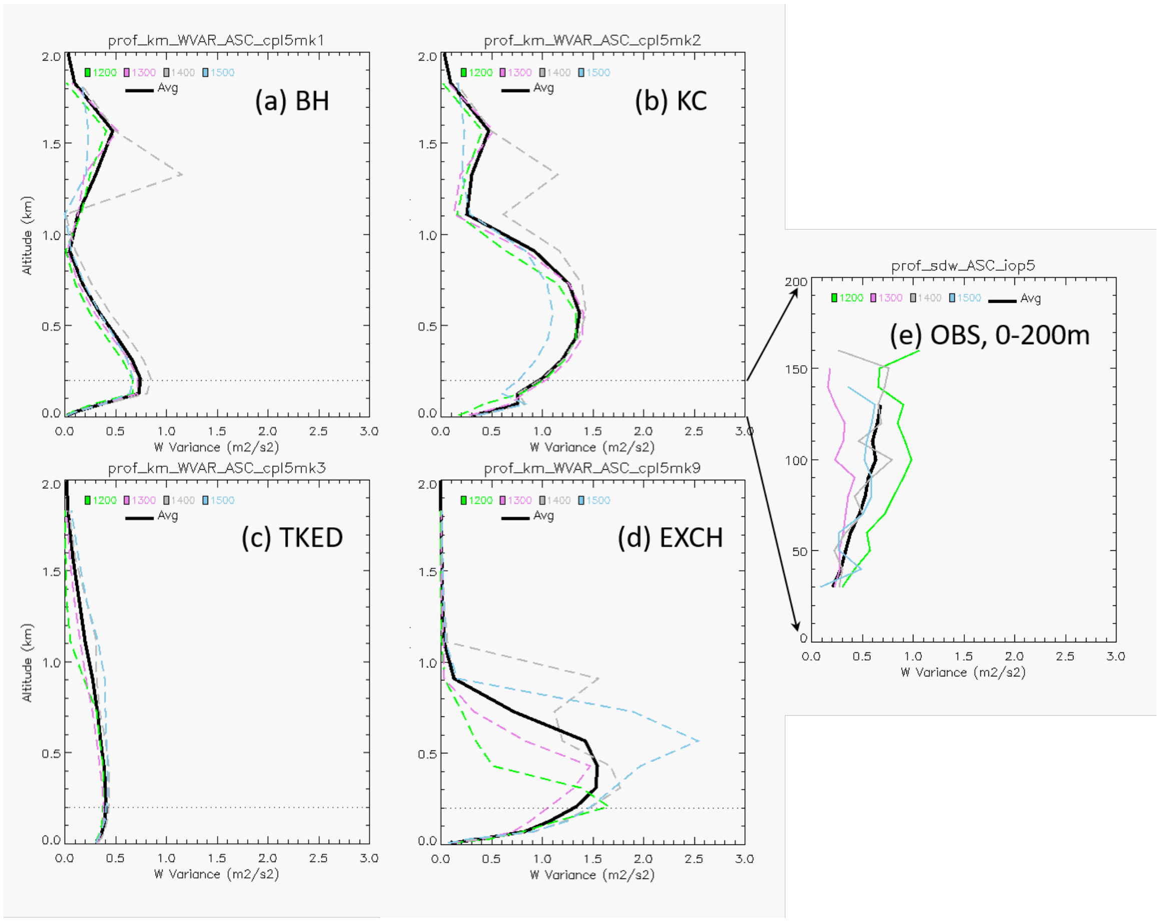

Figure 4 The same as Figure 2 but for IOP 5, 12 – 15 MST on October 18th, 2013.

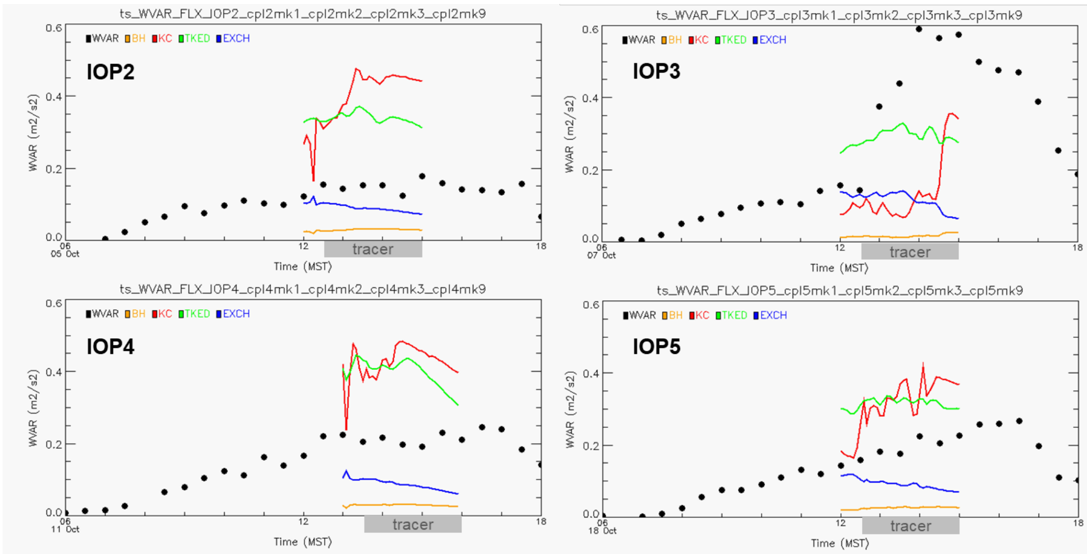

Figure 5 Time series of observed and modeled vertical velocity variance from HYSPLIT. The measurements were taken at the FLX station at 3.2 m height and modeled values were at 1st model layer at 10 m.

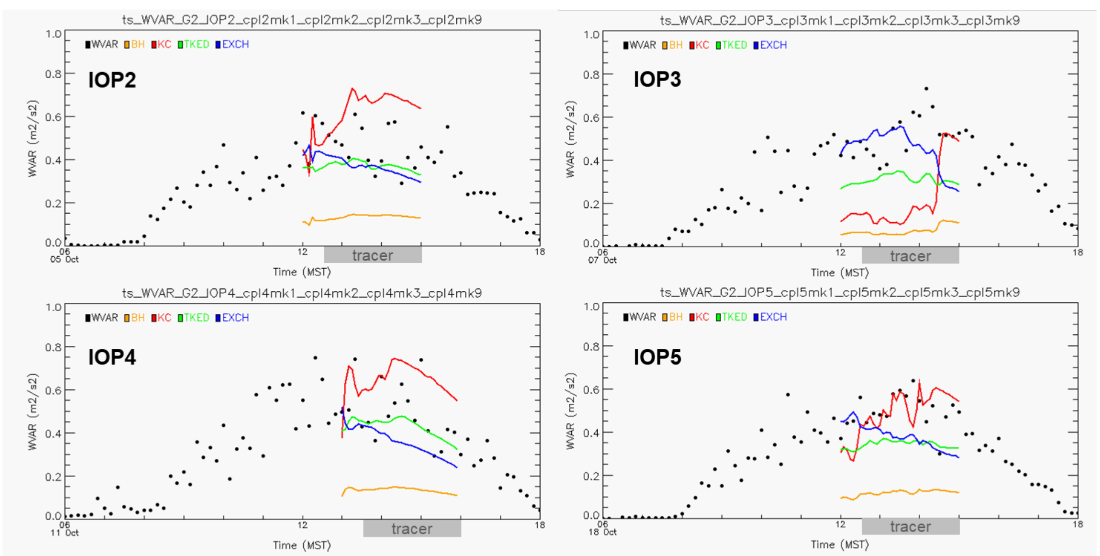

Figure 6 The same as Figure 5, except the measurements were taken at the GRI station at 30 m height and the modeled values were at 2nd model layer at 30 m.

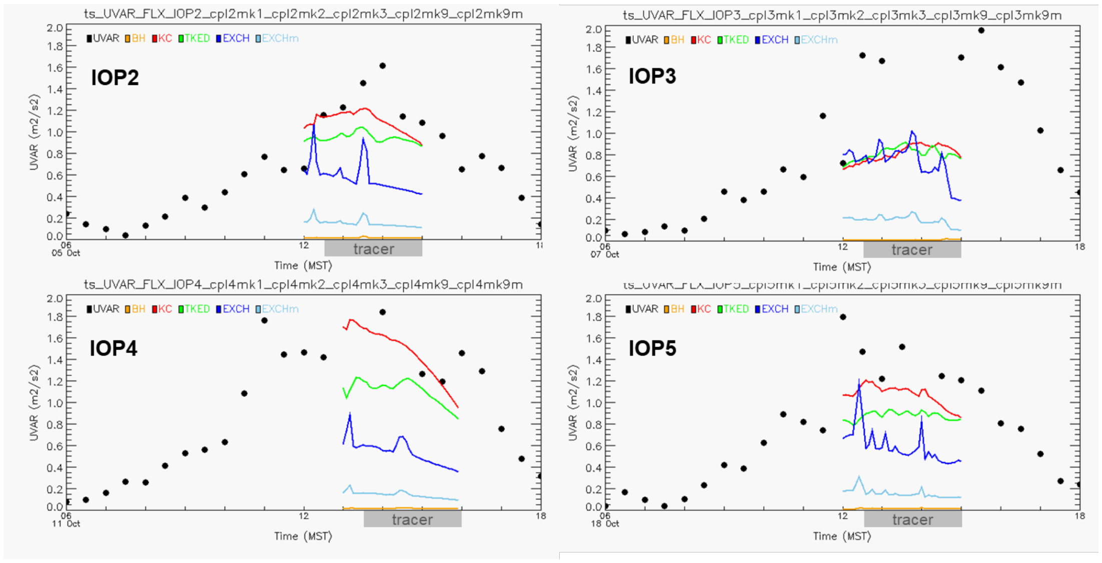

Figure 7 The same as Figure 5, except for the horizontal velocity variance.

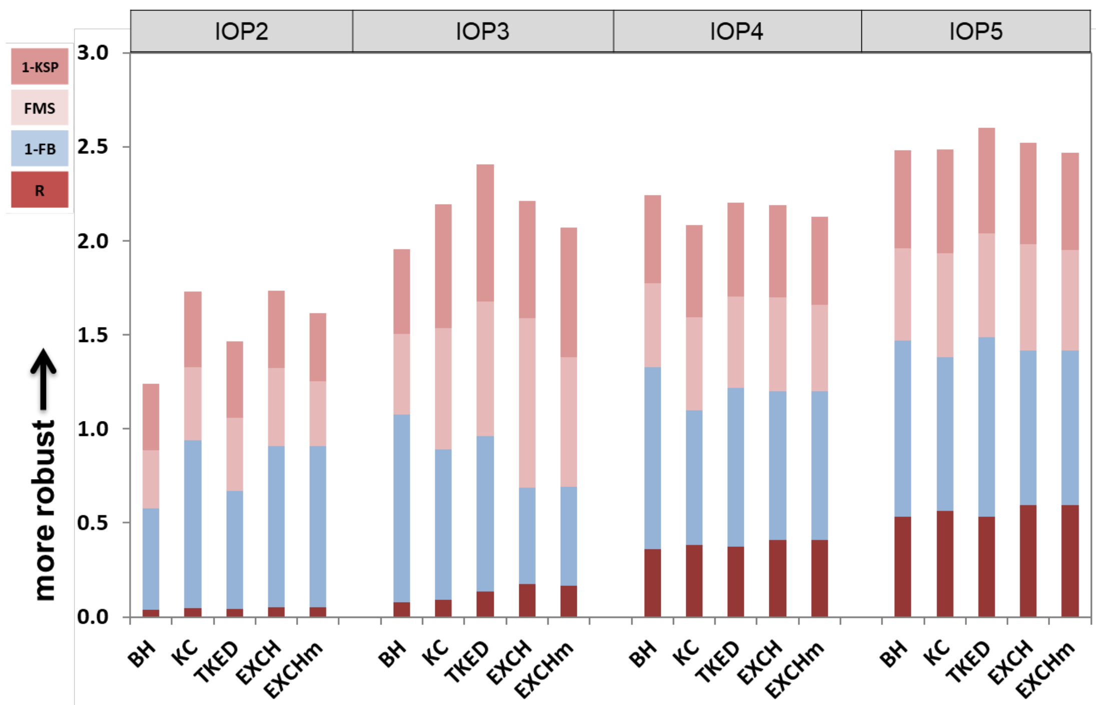

Figure 8 The statistical Rank of HYSPLIT results using different mixing options.

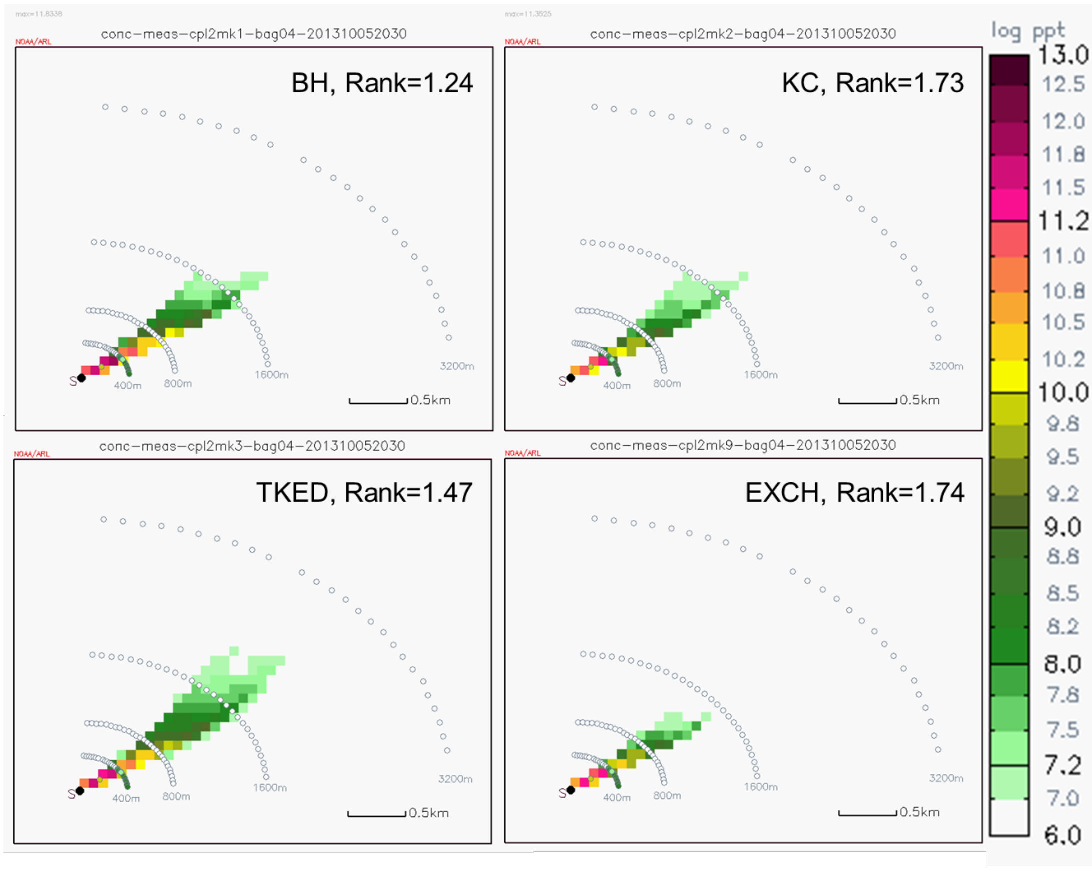

Figure 9 Tracer concentration plots for IOP 2 at 2030 UTC on October 5th, 2013 from HYSPLIT simulations using different mixing options. The shaded color is model concentrations while color-coded circles are measured concentrations. Rank of each simulation is noted in each panel. Unit: log ppt.

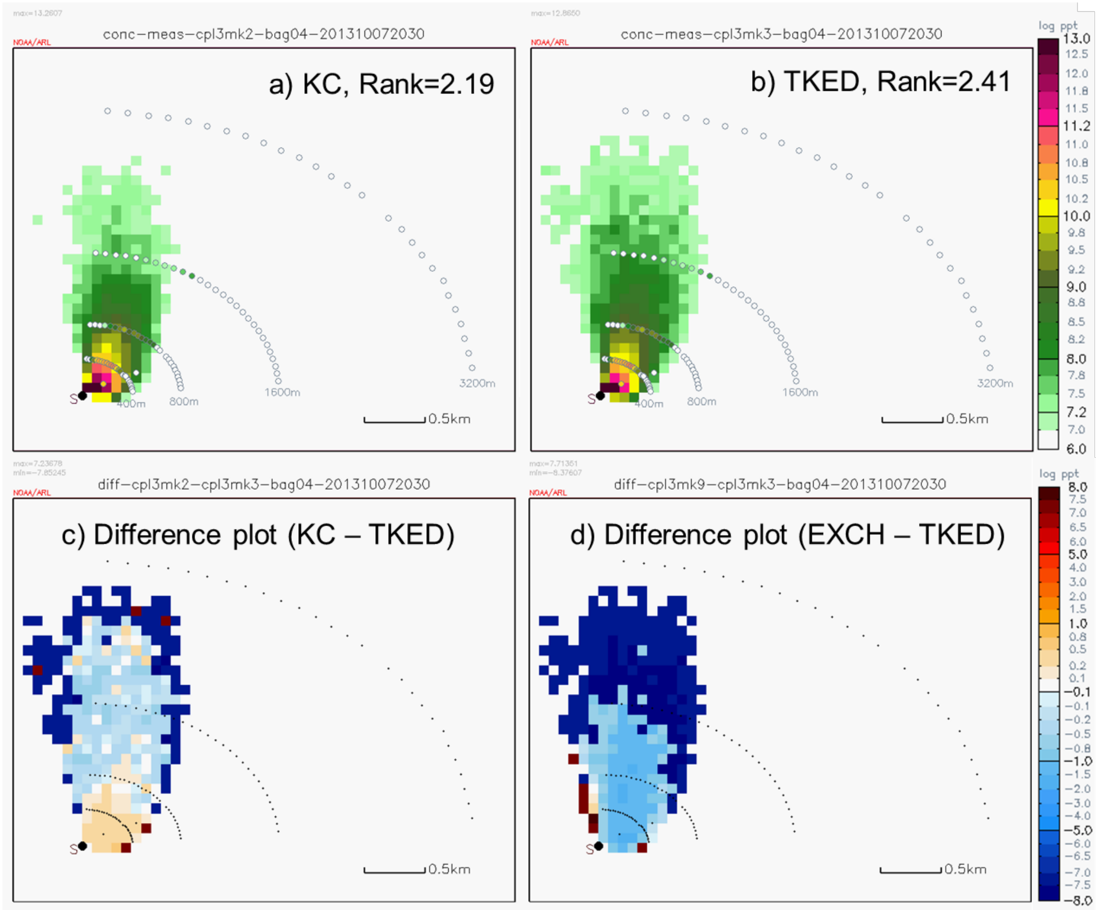

Figure 10 Tracer concentration plots for IOP 3 at 2030 UTC on October 7th, 2013 from HYSPLIT simulations using the KC (a) and TKED (b) mixing option. The shaded color is model concentrations while color-coded circles are measured concentrations. Rank of each simulation is noted in panel (a) and (b). Unit: log ppt. (c) and (d) Difference plot of tracer concentrations.

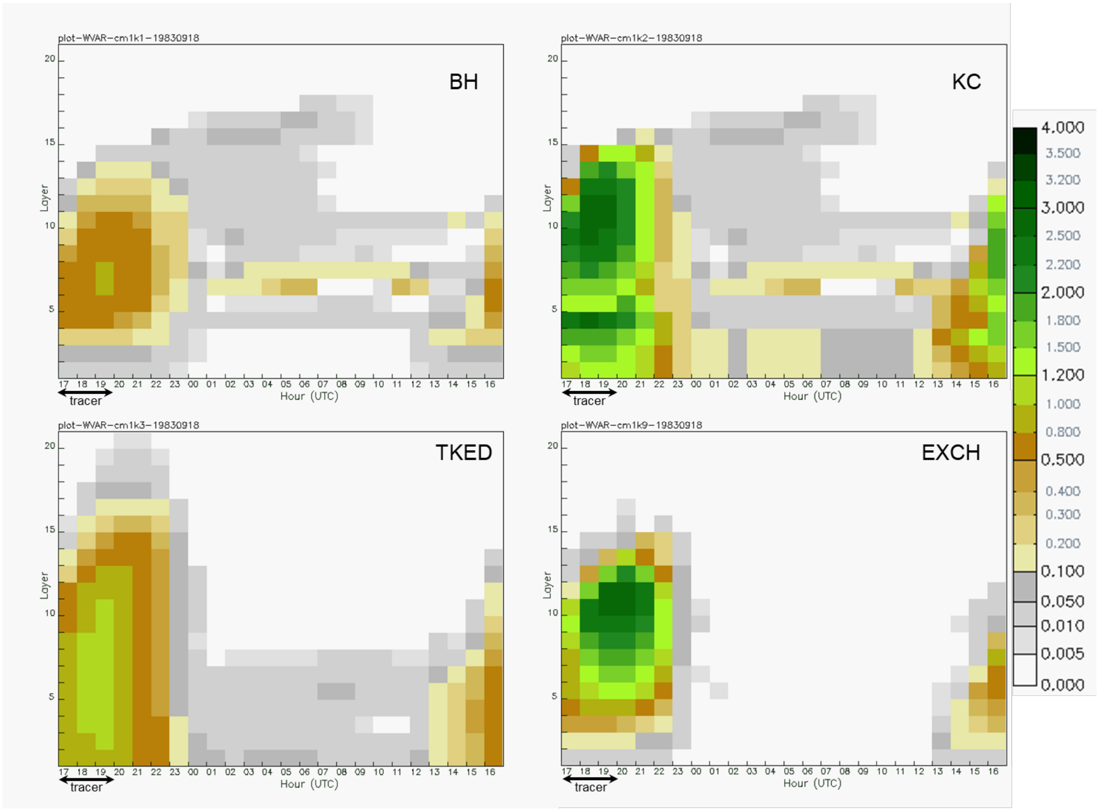

Figure 11 Time series of vertical velocity variance profiles from HYSPLIT using different mixing options for September 18th 17 UTC – 19th 16 UTC, 1983 (CAPTEX 1). Unit: m^2s^{-2}.

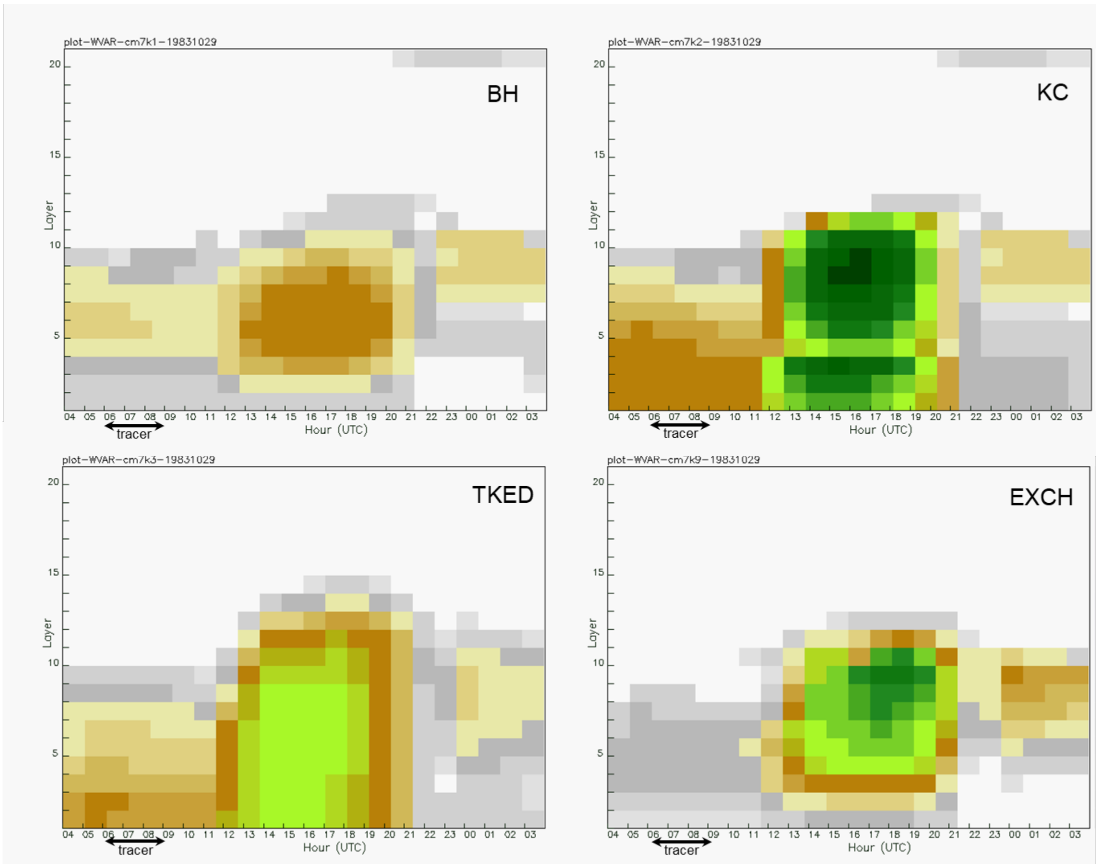

Figure 12 The same as Figure 11, expect for October 29th 04 UTC – 30th 03 UTC, 1983 (CATPEX 7).

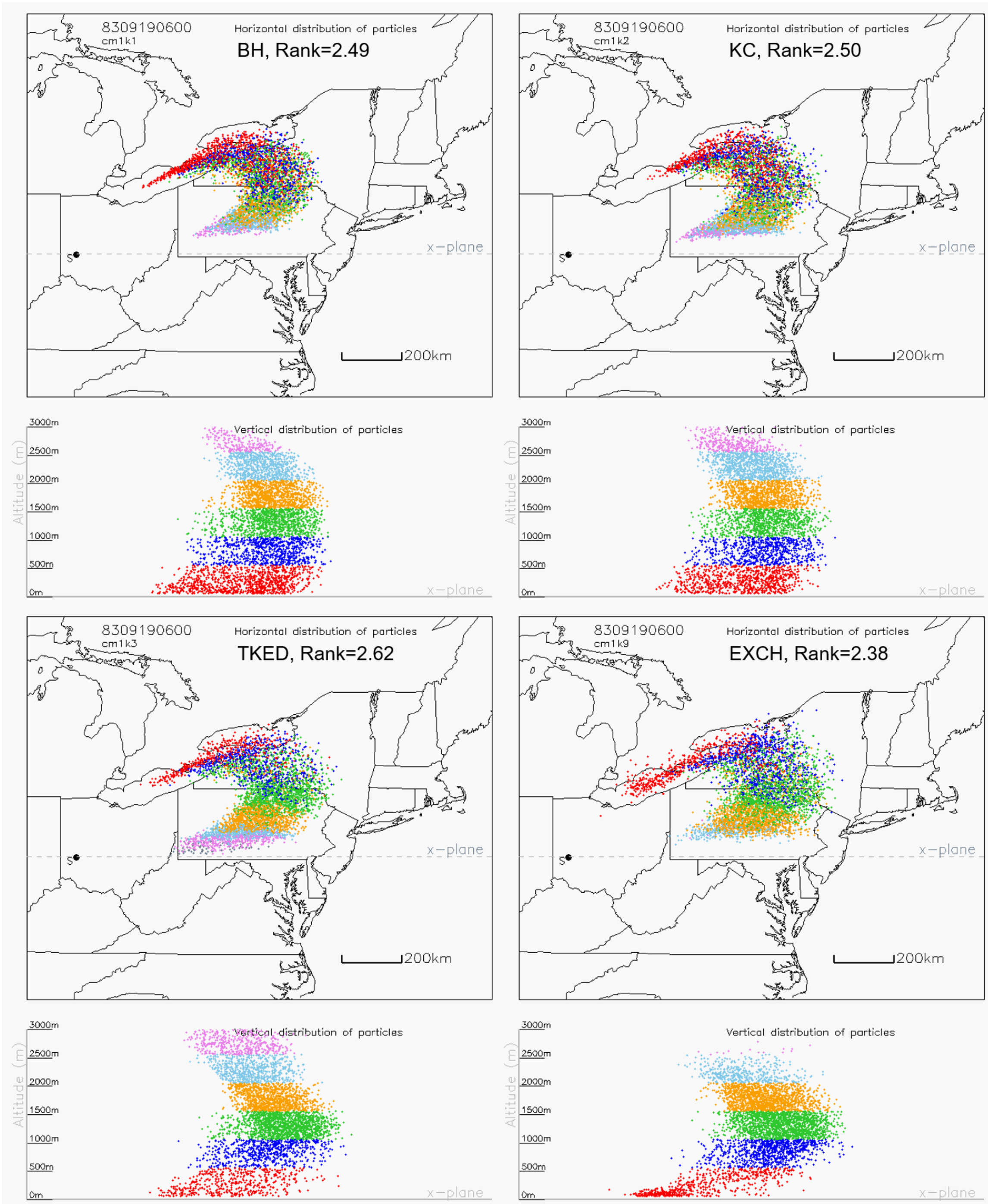

Figure 13 Horizontal and vertical distribution of particles simulated by HYSPLIT using different mixing options at September 19th 06 UTC, 1983 (CAPTEX 1). Colors indicate particles at different altitudes. Rank of each simulation is noted in each panel.

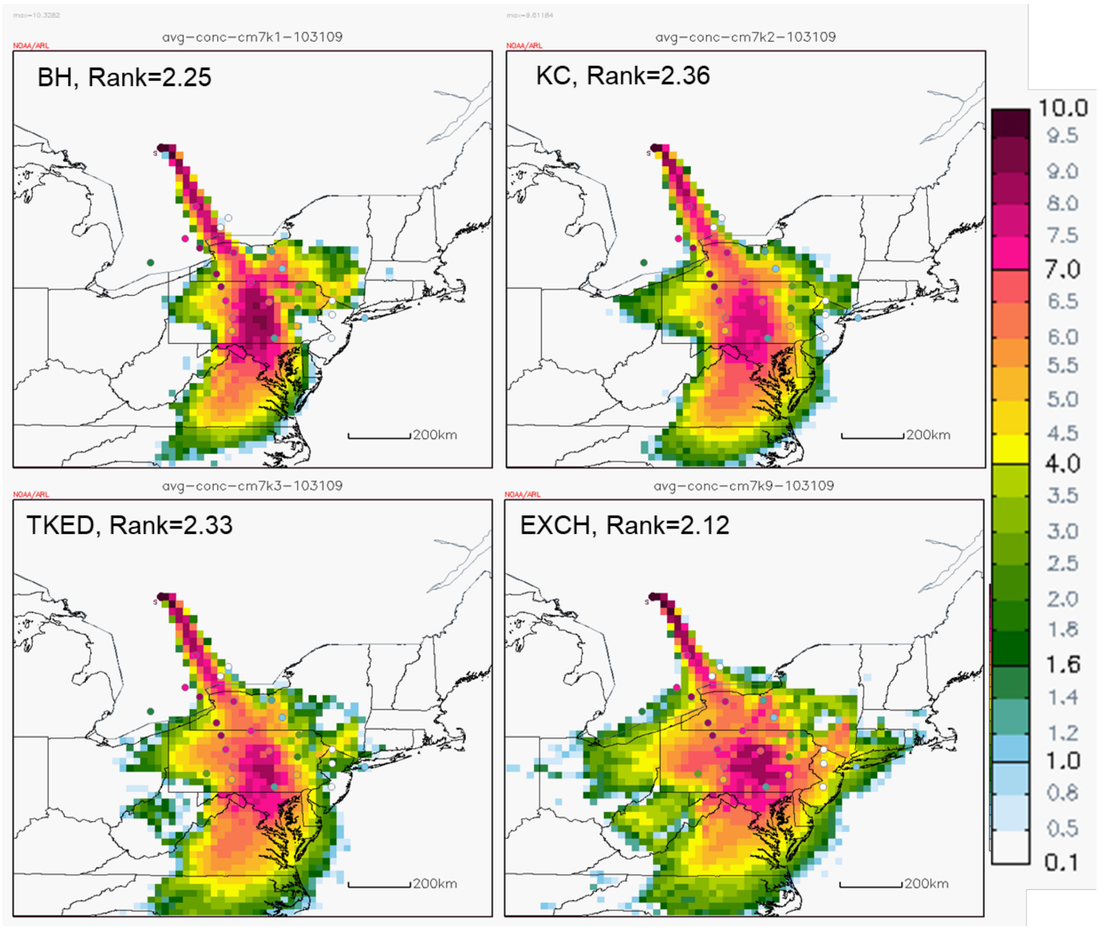

Figure 14 Tracer concentration plots for CAPTEX 7 from HYSPLIT simulations using different mixing options. The shaded color is 48-hour averaged model concentrations while color-coded circles are measured concentrations. Rank of each simulation is noted in each panel. Unit: log(pg/m^{-3}).